

# Advective spreading of storm-induced inertial oscillations in a model of the northwest Atlantic Ocean

Xiaoming Zhai, Richard J. Greatbatch and Jinyu Sheng

Department of Oceanography, Dalhousie University, Halifax, NS, Canada, B3H 4J1

## Abstract.

The spreading of inertial oscillations induced by the passage of Hurricane Juan (2003) across the Gulf Stream and the Scotian Shelf is examined using a regional model of the northwest Atlantic Ocean. It is found that surface-intensified inertial oscillations develop at locations remote from the storm track after a period of 5-10 days. A diagnostic technique reveals the importance of advection by the background geostrophic flow for explaining this effect. The results suggest that advection by mean circulation can play a role in redistributing near-inertial energy in the ocean. We argue that advective redistribution could have important consequences for understanding diapycnal mixing in the ocean.

## 1. Introduction

The upper ocean response to a moving storm has been studied observationally (e.g., *Leipper* [1967], *Brink* [1989] and *Dickey et al.* [1998]) and numerically (e.g., *Chang and Anthes* [1978], *Price* [1981], *Greatbatch* [1983], *Bender and Ginis* [2000]). The response is characterized by sea surface temperature (SST) cooling, and inertial oscillations that are most energetic to the right of the storm track. *Greatbatch* [1983] showed that on a time scale of a few inertial periods, the horizontal pressure gradients are small compared with the Coriolis terms for “large”, “fast” storms (that is “large” in the sense that the scale of the storm is large compared to the internal Rossby radius of deformation, and “fast” in the sense that the translation speed of the storm is large compared to the baroclinic gravity wave speed). The dominant balance is then between the acceleration terms and the Coriolis terms, resulting in inertial oscillations. The horizontal pressure gradient terms are crucial, however, to the dispersion of energy by inertial-gravity waves away from the storm track in the geostrophic adjustment process, and can not be neglected on time scales characteristic of that process (*Greatbatch* [1983]). *Gill* [1984] showed that the inertial energy propagates both horizontally and vertically as different vertical modes separate out from the storm track. On a  $\beta$ -plane, inertial oscillations generated at a particular latitude can propagate equatorward due to beta-dispersion (*Anderson and Gill* [1979]; *Garrett* [2001]). Data from moorings agree to some extent with the idea of the deep equatorward propagation of inertial oscillations (see *Chiswell* [2003] and *Alford* [2003a]). However, most previous studies do not consider the interaction between the inertial oscillations

and the background flow. *Kunze* [1985] showed that for near-inertial waves propagating in geostrophic shear, the horizontally nonuniform relative vorticity has the same effect as the  $\beta$ -effect on the near-inertial waves. As a consequence, these waves can be trapped in regions of negative vorticity (see also *D’Asaro* [1995]). *Davies and Xing* [2002] showed that the existence of the coast and the presence of density fronts influences the distribution of inertial energy and the propagation of near-inertial internal waves. *Xing and Davies* [2002] examined the non-linear interaction between inertial oscillations and internal tides and argued that non-linear interaction represents an important contribution to the energy cascade into higher frequency waves and eventually mixing. In this letter, we show the importance of geostrophic advection, rather than wave processes, for carrying inertial energy away from the storm track to remote regions in a model of the northwest Atlantic Ocean.

## 2. The model

We use the northwest Atlantic Ocean model developed by *Sheng et al.* [2001], which covers the area between 30°W and 76°W and between 35°N and 66°N with a horizontal resolution of one third degree in longitude. There are 31 unevenly spaced z levels with the centers of the top five levels located at 5, 16, 29, 44 and 61 m, respectively. A spin-up of 600 days using seasonally varying climatological forcing is used to allow the model to reach a quasi-equilibrium state before the storm forcing is introduced. The semi-prognostic method introduced by *Sheng et al.* [2001] is used to adjust the model momentum equations to correct for systematic errors during the spin-up period (see *Greatbatch et al.* [2004] for an overview). The end of the spin-up corresponds to early September.

To specify the storm forcing, we use Hurricane Juan from September 2003. Juan formed near Bermuda and then tracked northward across the Gulf Stream and the Scotian Shelf, making landfall at Halifax, Nova Scotia, as a category 2 hurricane. The wind stress for the storm is specified following *Chang and Anthes* [1978] as

$$\tau = \tau_{max} \times \begin{cases} r/r_{min} & 0 \leq r \leq r_{min} \\ (r_{max} - r)/(r_{max} - r_{min}) & r_{min} \leq r \leq r_{max} \\ 0 & r \geq r_{max} \end{cases} \quad (1)$$

where  $\tau$  is the amplitude of tangential wind stress with respect to the storm center, and  $r$  is the radial distance from the center. Here, we put  $r_{min} = 30$  km,  $r_{max} = 300$  km, and  $\tau_{max} = 3$  N m<sup>-2</sup>. The realistic storm track of Juan compiled by the National Hurricane Center is used in this study. Only wind stress forcing due to the storm is used to force the model; the surface buoyancy forcing due to the storm is not considered and has been shown elsewhere (e.g., *Price* [1981]) to be small in its effect. During the period of storm forcing, the vertical mixing scheme is modified from that used by *Sheng et al.* [2001]

to include entrainment at the base of the mixed layer due to shear instability based on a bulk Richardson number formulation following *Price et al.* [1986] (see *Zhai* [2004], for details). Two model runs are conducted using the end of the spin-up as the initial condition. The first (Run 1) has the storm forcing added to the climatological forcing, the second (Run 2) uses climatological forcing only. In addition, both these model runs are repeated, including the spin-up, with the density field specified from climatology (Runs 3 and 4, respectively). The difference between Runs 1 and 2, and between Runs 3 and 4, is used to represent the ocean response to the wind stress associated with the storm.

### 3. Model Results

Run 1 yields a reasonable oceanic response to the hurricane, including the rightward bias of the SST cooling, inertial oscillations in the wake and the generation of shelf waves on the eastern Canadian shelf (see Figure 1; details can be found in *Zhai* [2004]). In this letter, we focus on the onset of inertial oscillations (Figures 2a,b) after day 10 at Point 1 shown in Figure 1, a location far from the storm track and beyond the influence of the direct forcing by the storm. The horizontal velocity differences at this point are almost zero during the first 10 days (Figure 2a). After day 10, significant oscillations set in at the local inertial frequency with an amplitude of about  $5 \text{ cm s}^{-1}$ . There are two competing hypotheses concerning the mechanism for the onset of the inertial oscillations at Point 1: linear wave dispersion of inertial-gravity waves from the storm track (e.g. *Gill* [1984]) and advective processes (as noted by *D'Asaro* [1995]).

We use Runs 3 and 4 to determine the main process responsible for the appearance of the inertial oscillations at Point 1. Since the density field is specified from climatology in these runs, the horizontal pressure gradients are independent of the model-calculated temperature and salinity fields so that the baroclinic dispersion of inertial-gravity waves is excluded. Advection by the geostrophic flow associated with the climatology is nevertheless retained. (*Eden and Greatbatch* [2003] use a similar approach to diagnose the role of advection in the dynamics of a decadal oscillation in a model of the North Atlantic). Inertial oscillations now appear after day 17 (Figures 2c,d) and can only have been transported to Point 1 by geostrophic advection. The appearance of the inertial signal in the diagnostic run (Run 3) several days later than in Figure 2a can be explained by the different background (or advective) currents in Runs 1 and 2 compared with Runs 3 and 4.

In order to extract energy at the near-inertial frequency, a bandpass filter centered at the local ( $41^\circ\text{N}$ ) inertial frequency is used. The kinetic energy of the surface currents (Run 1 minus Run 2), given by  $(u^2 + v^2)/2$  (where  $u$  and  $v$  are the horizontal velocities) is computed after the bandpass filter is applied. The temporal and spatial evolution of the near-inertial energy at the sea surface is shown in Figure 3. The near-inertial energy is biased to the right of the storm track at day 6, due to the rightward bias in the storm-generated currents (e.g. *Price* [1981]). The near-inertial energy is then advected gradually by the Gulf Stream to the east at the latitude around  $41^\circ\text{N}$  (Figures 3b,c,d). The near-inertial energy decays as it is advected horizontally, due to dissipation and the vertical propagation of the energy. The time scale of the horizontal advection is consistent with the velocity scale for the Gulf Stream in the model. The shelf-break jet also advects the near-inertial energy to the southwest along the shelf-break as seen in Figure 3.

The near-inertial energy generated by the storm is initially confined in the mixed layer. It gradually propagates downward in the following ten days mainly on the right side of the

storm track, where there exists a larger energy source in the mixed layer (Figures 4a,b,c). The vertical propagation of the near-inertial energy can be interpreted using the concept of modal interference and separation as described in *Gill* [1984] and *Zervakis and Levine* [1995]. The total near-inertial energy decreases with time due to dissipation and only a small amount is left at day 18, which is advected eastward by the Gulf Stream from its source region on the right side of the storm track (Figure 4d).

### 4. Discussion

The thermohaline circulation of the ocean results primarily from deep water formation at sites in the Nordic and Labrador Seas, and around Antarctica, and upwelling throughout the rest of the global ocean. Mechanical energy input from the wind and tides is thought to be necessary to generate the diapycnal mixing required to support the upwelling branch of the thermohaline circulation (*Munk and Wunsch* [1998], *Wunsch* [2002]). A large part of the wind-induced energy flux goes to generate near-inertial oscillations in the mixed layer. Global maps of the wind-induced energy flux to inertial motions have been drawn by *Watanabe and Hibiya* [2002] and *Alford* [2003b]. Wind-induced inertial energy is believed to be redistributed by the propagation of inertial-gravity waves to lower latitudes, for example by the beta-dispersion effect (see *Alford* [2003a]). Our model results suggest that geostrophic advection could also play a role in redistributing inertial energy in the ocean. Furthermore, geostrophic advection could carry inertial energy to higher, rather than lower latitudes, where we speculate significant mixing could take place. (For example, near-inertial oscillations could be transported poleward of their turning latitude). Since a given energy level at higher latitudes causes much more mixing than at lower latitudes (*Gregg et al.* [2003], *Garrett* [2003]), mechanisms for transporting inertial energy to higher latitudes could be important for understanding mixing in the ocean.

### 5. Summary

We have reported on the spreading of storm-induced inertial oscillations in a model of the northwest Atlantic Ocean. Forcing mimicking the passage of Hurricane Juan in September 2003, as Juan crossed the Gulf Stream and the Scotian Shelf, was used to drive the model. We noted the onset, about 10 days after the storm, of inertial oscillations in regions far away from the storm track. A diagnostic technique, following *Eden and Greatbatch* [2003], was used to show the importance of geostrophic advection for carrying the inertial energy to regions remote from the storm track. The temporal evolution of the near-inertial energy isolated by a bandpass filter shows that the near-inertial energy spreads horizontally and vertically away from the storm track. It is advected mainly by two currents, the Gulf Stream and the shelf-break jet. This advective process, together with the long-range propagation of internal gravity waves, could be important for the global redistribution of wind-induced inertial energy in the ocean, and subsequently for the determining the global distribution of diapycnal mixing.

### Acknowledgments

We wish to thank Jian Lu (GFDL), Youyu Lu (BIO) and Chris Fogarty (MSC) for helpful discussions. This project is supported by funding from CFCAS.

## References

- Alford, M.H., Redistribution of energy available for ocean mixing by long-range propagation of internal waves, *Nature*, *423*, 159-162, 2003a.
- Alford, M.H., Improved global maps and 54-years history of wind-work on ocean inertial motions, *Geophys. Res. Lett.*, *30*(8), 1424, doi:10.1029/2002GL016614, 2003b.
- Anderson, D.L.T., and A.E. Gill, Beta dispersion of inertial waves, *J. Geophys. Res.*, *84*, 1836-1842, 1979.
- Bender, M.A., and I. Ginis, Real-case simulations of hurricane-ocean interaction using a high-resolution coupled model: effects on hurricane intensity, *Monthly Weather Review*, *128*, 917-946, 2000.
- Brink, K.H., Observations of the response of thermocline currents to a hurricane, *J. Phys. Oceanogr.*, *19*, 1017-1022, 1989.
- Chang, S.W., and R.A. Anthes, Numerical simulations of the ocean's nonlinear baroclinic response to translating hurricanes, *J. Phys. Oceanogr.*, *8*, 468-480, 1978.
- Chiswell, S.M., Deep equatorward propagation of inertial oscillations, *Geophys. Res. Lett.*, *30*, 1533-1536, 2003.
- Davies, A.M., and J. Xing, Influence of coastal fronts on near-inertial internal waves, *Geophys. Res. Lett.*, *29*, 2114-2117, 2002.
- D'Asaro, E.A., Upper-ocean inertial currents forced by a strong storm. Part III: Interaction of inertial currents and mesoscale eddies, *J. Phys. Oceanogr.*, *25*, 2953-2958, 1995.
- Dickey, T., D. Frye, J. McNeil, D. Manov, N. Nelson, D. Sigurdson, H. Jannasch, D. Siegel, T. Michaels and R. Johnson, Upper-ocean temperature response to hurricane Felix as measured by the Bermuda tested mooring, *Mon. Wea. Rev.*, *126*, 1195-1201, 1998.
- Eden, C., and R.J. Greatbatch, A damped decadal oscillation in the North Atlantic climate system, *J. Climate*, *16*, 4043-4060, 2003.
- Garrett, C., What is the "Near-Inertial" band and why is it different from the rest of the internal wave spectrum, *J. Phys. Oceanogr.*, *31*, 962-971, 2001.
- Garrett, C., Mixing with latitude, *Nature*, *422*, 477-478, 2003.
- Gill, A.E., On the behavior of internal waves in the wake of storms, *J. Phys. Oceanogr.*, *14*, 1129-1151, 1984.
- Greatbatch, R.J., On the response of the ocean to a moving storm: The nonlinear dynamics, *J. Phys. Oceanogr.*, *13*, 357-367, 1983.
- Greatbatch, R.J., J. Sheng, C. Eden, L. Tang, X. Zhai, and J. Zhao, The semi-prognostic method, *Cont. Shelf Res.*, in press, 2004.
- Gregg, M.C., T.B. Sanford, and D.P. Winkel, Reduced mixing from the breaking of internal waves in equatorial waters, *Nature*, *422*, 513-515, 2003.
- Kunze, E., Near-inertial propagation in geostrophic shear, *J. Phys. Oceanogr.*, *15*, 544-565, 1985.
- Leipper, D.F., Observed ocean conditions and hurricane Hilda (1964), *J. Atmos. Sci.*, *24*, 182-196, 1967.
- Munk, W., and C. Wunsch, Abyssal recipes II, Energetics of tidal and wind mixing, *Deep Sea Res., Part I*, *45*, 1977-2010, 1998.
- Price, J.F., Upper ocean response to a hurricane, *J. Phys. Oceanogr.*, *11*, 153-175, 1981.
- Price, J.F., R.A. Weller, and R. Pinkel, Diurnal cycling: Observations and models of the upper ocean response to diurnal heating, cooling, and wind mixing, *J. Geophys. Res.*, *91*, 8411-8427, 1986.
- Sheng, J., R. J. Greatbatch, and D. G. Wright, Improving the utility of ocean circulation models through adjustment of the momentum balance, *J. Geophys. Res.*, *106*, 16,711-16,728, 2001.
- Watanabe, M., and T. Hibiya, Global estimates of the wind-induced energy flux to inertial motions in the surface mixed layer, *Geophys. Res. Lett.*, *29*(8), 1239, doi:10.1029/2001GL014422, 2002.
- Wunsch, C., What is the thermohaline circulation? *Science*, *298*, 1179-1181, 2002.
- Xing, J., and A.M. Davies, Processes influencing the non-linear interaction between inertial oscillations, near inertial internal waves and internal tides, *Geophys. Res. Lett.*, *29*, 1067-1070, 2002.
- Zervakis, V., and M.D. Levine, Near-inertial energy propagation from the mixed layer: Theoretical consideration, *J. Phys. Oceanogr.*, *25*, 2872-2889, 1995.
- Zhai, X., Studying storm-induced circulation on the Scotian Shelf and slope using a two-way nested-grid model, M.Sc. thesis, Dalhousie University, 2004.

---

R. J. Greatbatch, J. Sheng and X. Zhai, Department of Oceanography, Dalhousie University, Halifax, NS, Canada, B3H 4J1. (Xiaoming.Zhai@phys.ocean.dal.ca)

(Received \_\_\_\_\_)

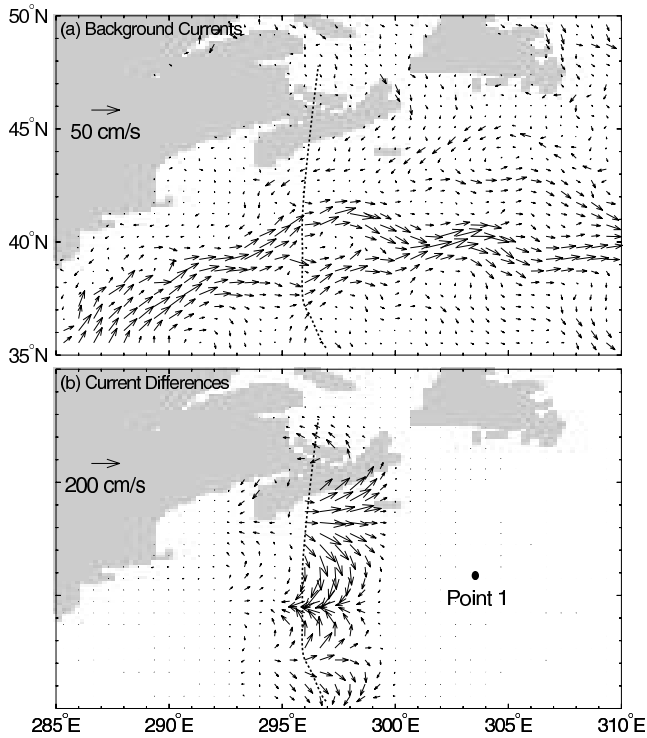


**Figure 1.** (a) The surface flow field at day 0 immediately before Hurricane Juan arrives; (b) the surface velocity differences between the model runs with and without Juan (Run 1 minus Run 2) at day 6. The storm track is represented by the dotted line. The bullet indicates the position of Point 1.

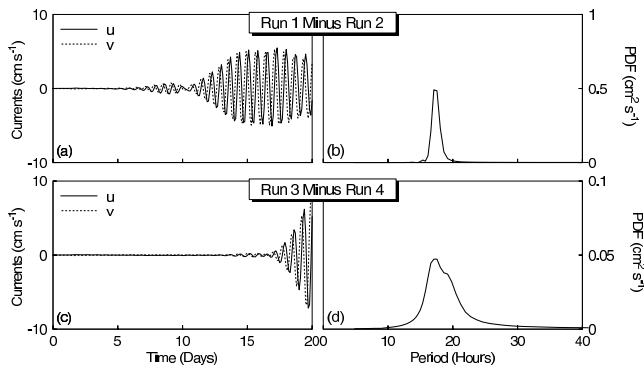


**Figure 2.** (a) Time series of the horizontal velocity differences between Run 1 and Run 2 at Point 1; (b) spectrum of the horizontal velocity differences between Run 1 and Run 2 at Point 1; (c) time series of the horizontal velocity differences between Run 3 and Run 4 at Point 1; (d) spectrum of the horizontal velocity differences between Run 3 and Run 4 at Point 1. Note the spectral peak near the local inertial period of about 18 hours.

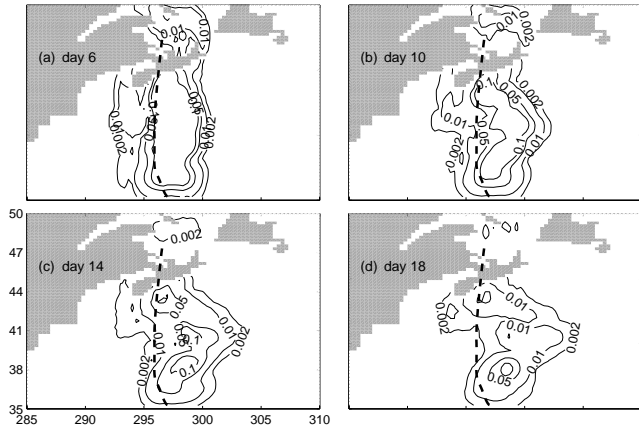


**Figure 3.** Temporal evolution of the near-inertial energy at the sea surface (unit:  $\text{m}^2 \text{s}^{-2}$ ). The dashed line represents the storm track.

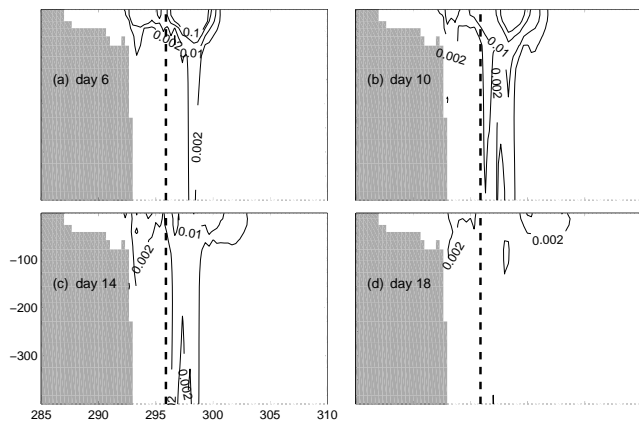


**Figure 4.** Vertical transect showing the temporal evolution of the near-inertial energy (unit:  $\text{m}^2 \text{s}^{-2}$ ) in the upper 400 m. The dashed line shows where the storm center intersects the transect.